2013 4th International Conference on Intelligent Systems, Modelling and Simulation

Classification of Vehicles Using Magnetic Field Angle Model

G.V. Prateek, Kolleri Nijil and K.V.S. Hari
Statistical Signal Processing Lab
Department of ECE
Indian Institute of Science
Bangalore, India
Email: {prateekgv,nijil,hari}@ece.iisc.ernet.in

***Abstract*—This paper presents an efficient approach to the modeling and classification of vehicles using the magnetic signature of the vehicle. A database was created using the magnetic signature collected over a wide range of vehicles(cars). A sensor dependent approach called as Magnetic Field Angle Model is proposed for modeling the obtained magnetic signature. Based on the data model, we present a novel method to extract the feature vector from the magnetic signature. In the classification of vehicles, a linear support vector machine configuration is used to classify the vehicles based on the obtained feature vectors.**

***Keywords-Wireless Sensor Networks, Magnetometers, AMR Sensors, Vehicle Detection, Data Modeling, Support Vector Machines, Vehicle Classification*.**

I. Introduction

The data collected by urban planning and development bodies [1] reveal that a great deal of resources are wasted because of the road traffic congestion. The number of man hours wasted due to traffic delay and the amount of pollution are significantly huge. Therefore, there is a great demand for intelligent traffic systems which are capable of monitoring traffic to reduce delay and to smoothen the flow of vehicles. An important parameter of current traffic management systems is the task of vehicle detection and classification. Distinction between different classes of vehicles provides useful information about traffic statistics.

Current technologies that are used in the study of traffic statistics include Intrusive technologies such as Inductive loop, Pneumatic tube, Piezoelectric, Weight-In-Motion and Non-Intrusive technologies such as Microwave Radar, Infrared based systems, Video-Image processing, Passive acoustic system. Among all the technologies Induction loop and Video-Image are most widely used but they have a lot of disadvantages. The Induction loop sensor is big in size which makes it difficulty in maintenance and the Video-Image based sensors are costly with big influence of external light conditions. For maximizing the benefits from all these technologies, there must be a large scale deployment of these sensors on all major freeways and local streets.

Wireless Sensor Networks have a high level of flexibility in their deployment configuration. Since the sensor nodes can be placed virtually anywhere on the road as long as they are within communication range, customized configurations can be adopted for different applications and environments. This unique characteristic is a big advantage over all other surveillance technologies. These passive sensors are mounted on low power consuming wireless transceivers called motes, capable of communicating with each other and a base station. The sensors are also capable of sensing the magnetic field. Therefore, the field induced due to a large permeable object, like a vehicle, can be sensed. Different vehicles have different metallic components and configuration, which cause different perturbation curves in the presence of a homogeneous magnetic field. This allows us to extract unique characteristics from the recorded magnetic signature. By feeding these attributes to a Support Vector Machine (SVM) [2], the vehicle class [3] can be determined. This can be used as an information for design of automatic toll collection system, prediction of highway capacity, giving signal priority in traffic control system and pavement life estimation in pavement design.

Notation: Bold lower-case alphabets and alphabets with an arrow on top of them represent vectors. Alphabets mentioned in parentheses as a super-script represent the axis direction and are always lower-case letters. Alphabets mentioned as a sub-script represent time-stamp and are always lower-case letters. All upper-case alphabets mentioned represent constants.

In Section II, we present a sensor dependent model for modeling the magnetic signature. Based on this model, we propose an algorithm to extract the feature vector in Section III. The obtained feature vector is given to a linear SVM and the performance of the existing and proposed algorithms are studied in Section IV . Conclusions can be found in Section V.

II. Data Modeling

A. Data Collection

The magnetometer senses the magnetic signature of a vehicle whenever the flux lines associated with it is perturbed by a vehicle in its vicinity. HMC1502[4] is a dual-axis anisotropic magnetoresistance (AMR)[5] magnetometer. It is mounted on a TelosB[6] mote and together they constitute

2166-0662/13 $26.00 © 2013 IEEE
DOI 10.1109/ISMS.2013.60

the magnetometer setup. The orientation of the magnetometer is such that it records the Y and Z-axis components of the magnetic field.

Extensive data was collected over a wide range of vehicles. Table I lists out all the cars covered during the data collection and are grouped based on the length of the car. A total of 234 magnetic field readings in Y and Z-axis direction each, were captured. In later sections we will be using Table I to study the performance of the SVM classifier by varying the number of datasets used in training and testing the classifier.

Table I: Vehicle Magnetic Signature Database[7] grouped based on the length of the car

Car-type	Type 1	Type 2	Type 3	Type 4
Car Len. (in *meters*)	(3.0-3.5)	(3.5-4.0)	(4.0-4.5)	(>4.5)
Type of *Car(n), where n represents number of datasets Cars = 42 Sets = 89	[1]800(8) [1]Alto(2) [2]Matiz(3) [3]Santro(5) [1]Omni(6) [9]Spark(1) [4]Nano(2) [1]WagonR(4) [1]Estillo(3) [9]Beat(2) [13]Reva(1)	[11]Corsa(2) [3]i20(1) [5]Figo(2) [3]GetZ(2) [3]i10(4) [4]Indica(6) [7]Palio(1) [1]Swift(2) [1]Zen(2) [3]Ritz(1)	[3]Accent(1) [2]Cielo(1) [6]City(4) [12]Vento(1) [1]SX4(2) [3]Verna(1) [1]Esteem(2) [4]Indigo(2) [1]Dzire(1) [4]Sumo(1) [5]Fiesta(1) [6]Petra(1) [14]Logan(1)	[6]Civic(1) [8]Corolla(1) [3]Elentra(2) [8]Innova(2) [7]Linea(1) [3]Sonata(1) [10]Octiva(1) [10]Laura(1)
Number of Datasets	87	67	53	27

* Indicates the Car Manufacturer
[1] - Maruti Suzuki; [2] - Daewoo; [3] - Hyundai; [4] - Tata Motors; [5] - Ford; [6] - Honda; [7] - Fiat; [8] - Toyota; [9] - Chevrolet; [10] - Skoda; [11] - Opel; [12] - Volkswagon; [13] - Mahindra; [14] - Renault.

B. Proposed Sensor Dependent Model: Magnetic Field Angle Model (MFMA)

We propose a new model for modeling the magnetic signature of a vehicle. Depending on the metallic configuration and composition of a vehicle, different magnetic signatures are induced by different vehicles. An AMR Wheatstone bridge magnetometer is the most commonly used device in a wireless sensor node to detect the induced magnetic field. The four AMR elements are oriented in a diamond shape and the ends of the bridge are connected to a differential Op-Amp of a fixed voltage gain. The bridge becomes unbalanced in the presence of a ferrous material in the magnetic field. HMC1052 has two Wheatstone bridge setups in orthogonal directions and can be used to measure the component of the magnetic field along two orthogonal directions.

Let K be the material constant dependent on R_0 and ΔR_0 (Resistances of the AMR Element), G be the voltage gain of the differential Op-Amp to which the ends of the Wheatstone bridge are connected, V_s be the supply voltage and α be the angle between the internal magnetization vector and the direction of current called as rotation angle. Then, V_{BD} which is the amplified output of the Wheatstone bridge as seen by the differential Op-Amp is as follows:

$$V_{BD} = G\left(\frac{K}{1+K}\right)(\sin 2\alpha)V_s. \quad (1)$$

$$\implies \alpha = \frac{1}{2}\sin^{-1}\left(\frac{V_{BD}}{V_s}\left(1+\frac{1}{K}\right)\frac{1}{G}\right) \quad (2)$$

Refer Appendix A for the derivation of equation (1). From equation (2), we can say $\alpha \in \left[\frac{-\pi}{4}, \frac{+\pi}{4}\right]$. Now consider a vehicle moving on a straight road with constant velocity as shown in Fig. 1, with the HMC1502 sensor placed at the origin. As the vehicle approaches the sensor, the flux lines bend away from the sensor towards the vehicle due to the presence of metallic composition in the chassis of the vehicle. In other words, the number of flux lines passing through the surface of the permalloy of the HMC1502 sensor decreases. A change in the number of magnetic flux lines is equivalent to change in the induced magnetic field. This in-turn changes the angle between the internal magnetization vector and the direction of current of the anisotropic mangetoresistances, which makes the bridge unbalanced. The same theory holds true when the vehicle leaves the sensor. But, when the metallic content of the vehicle is aligned with the sensor, more and more flux lines pass through the surface of permalloy. As the number of flux lines increases, the induced magnetic field also increases. As a result, the angle between the internal magnetization vector and direction of current changes and the bridge becomes unbalanced. In this way the induced magnetic field is captured using an AMR Wheatstone bridge in a particular direction.

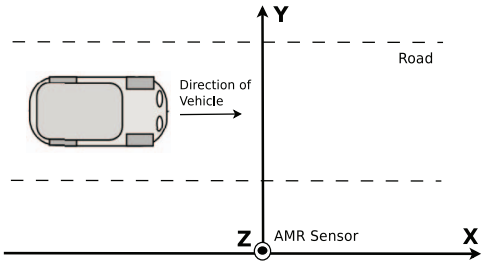

Figure 1: The AMR sensor is placed at the origin. Different magnetic signatures are induced by different vehicles.

Let g be a non-linear function with input α_k, where α_k is the angle between the internal magnetization vector and direction of current at kT_s time-instant. Let y_k be the measured output and η_k be the measurement noise at kT_s time-instant. In the signal processing framework, the sensor model can be defined as follows.

$$y_k = g(\alpha_k) + \eta_k$$
$$= G\left(\frac{K}{K+1}\right)\sin(2\alpha_k)V_s + \eta_k \quad (3)$$

In order to reduce sensor model error and the complexity of computing α at every time-instant, we assume α is constant

over a segment of length L. Let $\alpha(j)$ represents the rotation angle value in the j^{th} segment. With this assumption, we estimate the segmented α values based on Least Squares (LS) cost function.

$$\hat{\alpha}(j) = \arg\min_{\alpha(j)} \sum_{i=1}^{L} \left| y_{(j-1)L+i} - g(\alpha(j)) \right|^2, \quad (4)$$

$$\text{subject to } |\alpha(j)| \leq \frac{\pi}{4}, \text{where } j \in \{1, \cdots, \lfloor N/L \rfloor\}$$

The performance of the least squares cost function for different values of L is studied in the next section.

III. Feature Extraction

Vehicle Classification is the process of assigning each vehicle into a pre-defined vehicle class based on some features extracted from its magnetic signature. The feature vector is obtained by processing the obtained magnetic signature. We shall briefly discuss about the existing algorithms first and then, we propose an algorithm to obtain feature vector from the magnetic signature of a vehicle based on the MFAM studied in the previous section.

A. Average-Bar Transform[8]

Here the vehicle magnetic signature vector of length N, is divided into S sub-vectors. The mean value of each sub-vector is calculated and the obtained values for S sub-vector is the feature vector. The value of S is fixed for all classes of vehicles. The Z-axis measurements of the magnetometer are primarily used for feature extraction because of their localized character (perturbations in the magnetic field in presence of a vehicle are significant in Z-axis direction).

B. Hill-Pattern Transform[8]

This method transforms the signal into a sequence of $\{+1, -1\}$ and without losing much information. This extracts the pattern of "peaks" and "valleys" (local maxima and minima) of the input signal. The sequence of $\{+1, -1\}$ is used as a feature vector. In this case also the Z-axis measurements of the magnetometer are primarily used for feature extraction.

C. Magnetic Dipole Model[9]

In this method, a vehicle is modeled as an array of magnetic dipoles. The strength of the magnetic dipole and the separation between the magnetic dipoles varies for different vehicles.

D. Proposed Algorithm - Segmented Magnetic Field Angle Algorithm (SMFA Algorithm)

In this algorithm, we use the MFMA data model explained in section II-B to estimate the parameter $\hat{\boldsymbol{\alpha}} = [\alpha(1), \ldots, \alpha(j)]^T, j \in \{1, \ldots, \lfloor N/L \rfloor\}$ using the least squares cost function in equation (4), where α is the angle the magnetization vector makes with the current vector direction on the surface of the permalloy and L is the length of the segment. From the estimated $\hat{\boldsymbol{\alpha}}$, we obtain α_{max} and α_{min} which are the maximum and minimum value of $\hat{\boldsymbol{\alpha}}$ respectively, since the metallic composition and configuration of a vehicle is dependent on α_{max} and α_{min}. The higher the ferrous content in the vehicle, the larger the absolute values of α_{max} and α_{min}. Also, we obtain Q which is the number of non-zero bins of the histogram plot of $\hat{\boldsymbol{\alpha}}$, for a fixed bin-size W. The value Q is a good parameter which relates to the spread of the signal.

The induced magnetic field curve varies smoothly since the velocity of the vehicle is constant and is continuous. Considering these two observations, we compute the $\hat{\boldsymbol{\alpha}}$ for different segment lengths L. The value of α_{min} and α_{max} remains same for a fixed segment length L in spite of changing bin-size W of the histogram as seen in Table II. Also as L increases, the $RMSE$ value increases.

Table II: Features Extraction using SMFA Algorithm for a Tata Indica Car's Magnetic Signature

Seg. Len	α_{min}	α_{max}	Q for $W =$			$RMSE$
			1°	2.5°	5°	
$L = 2$	-15.71°	$+26.23^\circ$	26	11	6	2.15
$L = 4$	-15.49°	$+25.75^\circ$	20	11	6	4.78
$L = 6$	-14.76°	$+24.28^\circ$	17	10	5	7.30
$L = 8$	-15.03°	$+24.45^\circ$	13	9	5	9.62

The value of computing $\hat{\boldsymbol{\alpha}}$ is expensive as it involves computation of $\arcsin$ for every time-instant $k \in \{1, \ldots, \lfloor N/L \rfloor\}$. The larger the value of L, lesser is the computational cost. The computational complexity of the least square cost function shown in equation (4) is of the order $O(\lfloor N/L \rfloor)$. In order to check the variation of $RMSE$ as the segment length L increases, we calculate the average $RMSE$ for all the datasets mentioned in Table I across different values of $M \in \{1, 2, 3, 4\}$. Let D be the total number of datasets available ($D = 234$) and $RMSE_i$ be the $RMSE$ value for the i^{th} dataset, then the Average $RMSE$ denoted by $\overline{RMSE}$ is computed as follows.

$$\overline{RMSE} = \frac{1}{D} \sum_{i=1}^{D} RMSE_i \quad (5)$$

Table III shows the order of complexity and average $RMSE$ denoted by $\overline{RMSE}$ for $L \in \{2, 4, 6, 8\}$ for all the datasets available in Table I based on equation (5). As the value of L increases, the $\overline{RMSE}$ value increases. But, this does not help us in choosing a value of L on which the classification algorithm can be performed. In order to do that, we run the classifier algorithm and check for its performance across different segment lengths. The analysis of the performance measure is done in the next section.

IV. Classification Performance

In this section we look at classification of the vehicles mentioned in Table I based on the features obtained using MDMS algorithm. A SVM model usually involves separating data into sets - training and testing. It is built using

Table III: Computational Complexity and $\overline{RMSE}$ Across Available Datasets

Segment Length	Order of Complexity	$\overline{RMSE}$
$L=2$	$O(\lfloor N/2 \rfloor)$	1.967
$L=4$	$O(\lfloor N/4 \rfloor)$	3.381
$L=6$	$O(\lfloor N/6 \rfloor)$	4.689
$L=8$	$O(\lfloor N/8 \rfloor)$	5.905

Algorithm 1 Segmented Magnetic Field Angle Algorithm (SMFA Algorithm)

Input: Smoothed Vehicle Magnetic Signature - $a_{N\times 1}$

1: Subtract every $k^{th}, k \in \{1,\ldots,N\}$ sample with the mean of first $N/10$ samples of $a_{N\times 1}$

2: **for** j=1 to $\lfloor N/L \rfloor$ **do**

3: Estimate $\hat{\alpha}(j)$

$$\hat{\alpha}(j) = \arg\min_{\alpha(j)} \sum_{i=1}^{L} \left| a_{(j-1)L+i} - g(\alpha(j)) \right|^2$$

subject to $|\hat{\alpha}(j)| \leq \frac{\pi}{4}$

4: **end for**

Output: α_{min} = minimum of $\hat{\boldsymbol{\alpha}}$, α_{max} = maximum of $\hat{\boldsymbol{\alpha}}$, Q = no. of non-zero bins of $\hat{\boldsymbol{\alpha}}$ histogram for bin-size W.

the datasets that are used as training data. We are using SVM [2] for data classification. Each instance in a training set contains one label value and several attributes. The goal of the SVM is to produce a model (based on the training samples) which predicts the target label of the test sample given only the test sample attributes. Given a training set of instance-label pairs $(\mathbf{x}_i, s_i)$, $i = \{1,\ldots,F\}$ where $\mathbf{x}_i \in \mathbb{R}^P$, $\mathbf{s} \in \{1,-1\}^F$ and P is the length of the feature vector then, SVMs require the solution of the following optimization problem

$$\begin{aligned} \min_{\mathbf{w},\gamma,\boldsymbol{\xi}} \quad & \frac{1}{2}\mathbf{w}^T\mathbf{w} + C\sum_{i=1}^{F}\xi_i \\ \text{subject to} \quad & s_i(\mathbf{w}^T\Phi(\mathbf{x}_i)+\gamma) \geq 1-\xi_i, \\ & \xi_i \geq 0. \end{aligned} \tag{6}$$

The function Φ maps the training vectors into a higher dimensional space. SVM finds a linear separating decision hyperplane with the maximal margin in the higher dimensional space. $C > 0$ is the penalty parameter for the error term $\boldsymbol{\xi}$ with i^{th} element ξ_i. Furthermore, $K(\mathbf{x}_i,\mathbf{x}_j) \equiv \Phi(\mathbf{x}_i)^T\Phi(\mathbf{x}_j)$ is called the Kernel function. We used the MATLAB[10] function **svmtrain** to train SVM classifier. To classify new data with the result of the training data, MATLAB function **svmclassify**, which is a binary classifier, is used. In order to randomly pick training and testing data of lengths L_{tr} and L_{ts} respectively, MATLAB function **crossvalind** is used. This function takes in a parameter $q \in [0,1]$ as input which is used to control the lengths of training and testing data. In all our simulation results, we have considered a *linear kernel* function as it performed better than other kernel functions like polynomial kernel, Gaussian radial basis function kernel and hyperbolic tangent kernel.

If Ω_i is the number of vehicles classified correctly among L_{ts} number of cars in the i^{th} iteration and the total number of iterations is I, then using the SVM toolbox functions, the correct rate of classification, C_R across two different classes fixing the training data and testing data lengths is calculated as follows.

$$C_R = \frac{1}{I}\sum_{i=1}^{I}\frac{\Omega_i}{L_{ts}} \tag{7}$$

We begin our analysis by studying the performance of SMFA Algorithm. The feature vector includes minimum value, α_{min}; maximum value, α_{max}; and the number of non-zero bins Q, obtained from $\hat{\boldsymbol{\alpha}}$. Table IV shows the C_R value for different segment lengths, $L \in \{2,4,6,8\}$, across different bin-size W for Type 1 (length of the car lies between $3.0m$ to $3.5m$) vs Type 4 (length of the car lies between $4.5m$ to $5.0m$). The value of $I = 100$ is fixed in all our simulations and based on the C_R values obtained, the SVM performs the best for segment length of $L = 6$.

Table IV: Percentage of Correct Rate of Classification C_R for Type 1 vs Type 4 Cars Based on SMFA Algorithm

Dataset Length (L_{tr}, L_{ts})	Segment Length	Bin Size 1.0°	2.5°	5.0°
(70,44)	$L=2$	77.42	76.63	76.63
	$L=4$	77.92	77.16	77.67
	$L=6$	78.23	77.23	77.88
	$L=8$	77.60	77.86	78.37
(80,34)	$L=2$	76.55	76.21	77.18
	$L=4$	76.33	76.39	76.55
	$L=6$	77.00	77.03	77.76
	$L=8$	77.21	77.03	77.70
(90,24)	$L=2$	79.17	78.91	79.26
	$L=4$	79.17	78.87	79.09
	$L=6$	79.65	79.57	80.48
	$L=8$	79.78	79.78	80.09

Table V gives the C_R for different lengths of training and testing datasets of cars belonging to Type 1 and Type 4 category. The SVM performance of the existing algorithms is compared with the proposed feature extraction algorithms. Based on the values of C_R obtained in Table V, SMFA algorithm performs better than other algorithms. The SMFA algorithm gave 80.48% as the correct rate of classification for segment length $L = 6$ and bin-size $W = 5°$. Table VI gives the C_R for different lengths of training and testing datasets of cars belonging to Type 1 and Type 2 grouped together verses Type 3 and Type 4 grouped together. In this case also, the SMFA algorithm performs better than existing algorithms and MDMS algorithm. The SMFA algorithm gave 68.67% as the correct rate of classification for segment length $L = 6$ and bin-size $W = 5°$.

Table V: Percentage of Correct Rate of Classification C_R for Type 1 vs Type 4 Car for Average Bar, Hill Transform, MDMS Algorithm and SFMA Algorithm

Datasets	Feature Extraction Algorithms						
(L_{tr}, L_{ts})	Average Bar Algorithm[8]	Hill Transform Algorithm[8]	MDMS Algorithm[9]		SMFA Algorithm		
			3-DM Normalized Moments $\tilde{\mathbf{m}}$	3-DM Dipole Separation ΔX	Segment Length $L = 6$		
					$W = 1^\circ$	$W = 2.5^\circ$	$W = 5^\circ$
(70,44)	72.70	76.33	73.80	74.14	77.23	77.23	77.88
(75,39)	73.42	75.32	72.70	73.29	77.37	77.37	77.66
(80,34)	73.88	75.39	74.12	74.27	77.00	77.03	77.76
(85,29)	75.36	78.43	76.40	76.61	79.61	80.25	79.89
(90,24)	76.26	77.91	76.67	76.78	79.65	79.57	**80.48**

Table VI: Percentage of Correct Rate of Classification C_R for Type 1 & Type 2 vs Type 3 & Type 4 Car for Average Bar, Hill Transform, MDMS Algorithm and SFMA Algorithm

Datasets	Feature Extraction Algorithms						
(L_{tr}, L_{ts})	Average Bar Algorithm [8]	Hill Transform Algorithm [8]	MDMS Algorithm [9]		SMFA Algorithm		
			3-DM Normalized Moments $\tilde{\mathbf{m}}$	3-DM Dipole Separation ΔX	Segment Length $L = 6$		
					$W = 1^\circ$	$W = 2.5^\circ$	$W = 5^\circ$
(110,124)	61.74	63.88	63.25	63.55	67.28	67.56	67.47
(120,114)	62.79	64.27	63.97	64.16	67.94	67.89	67.90
(130,104)	63.28	64.73	63.32	63.71	68.04	67.57	68.31
(140,94)	62.80	64.42	63.30	63.61	67.85	67.18	68.04
(150,84)	63.00	64.37	63.95	64.31	68.27	68.23	**68.67**

V. Conclusion

The main contribution of this paper is proposing a sensor dependent data model called as the Magnetic Field Angle Model (MFAM). In this model, we modeled the magnetic signature of a vehicle based on the metallic configuration and composition of the vehicle. The angle between the internal magnetization vector and the direction of current for a fixed segment length is estimated using a least square cost function. In SMFA algorithm, from the estimated rotation angle values for different segment lengths, we obtain the maximum rotation angle, minimum rotation angle and the spread of the signal from the histogram plot of the estimated rotation angles. These three values are considered as a feature vector and a SVM configuration with linear kernel is applied. Based on the percentage of correct rate of classification obtained for different lengths of training and testing data, the SMFA algorithm performs better than all algorithms when there is a distinct difference between the length of the cars. Also the computational complexity of SMFA is lower as compared with the other algorithms.

Acknowledgments

This project is funded by DIT-ASTEC Wireless Sensor Project, Department of Information Technology, Ministry of Communications & Information Technology, Govt. of India.

Appendix A.
Differential Voltage Equation for AMR Wheatstone Bridge

If an external magnetic field H is applied, parallel to the plane of the permalloy but perpendicular to the current flow as shown in Fig. 2, the internal magnetization vector of the permalloy will rotate around an angle α. As a result, the resistance of R of the permalloy will change as a function of the rotation angle α and is as follows.

$$R = R_0 + \Delta R_0 \cos^2 \alpha \tag{8}$$

where R_0 and ΔR_0 are material constants. If H is the applied field and H_0 is the earth's magnetic field, then the value of α can be obtained using the following equation.

$$\sin^2 \alpha = \begin{cases} \frac{H^2}{{H_0}^2} & \text{for } H \leq H_0 \\ 1 & \text{for } H > H_0 \end{cases} \tag{9}$$

The Resistance of an AMR sensors is now given by:

$$R = \begin{cases} R_0 + \Delta R_0 \left(1 - \frac{H^2}{{H_0}^2}\right) & \text{for } H \leq H_0 \\ R_0 & \text{for } H > H_0 \end{cases} \tag{10}$$

The magnetoresistive effect can be linearized by depositing

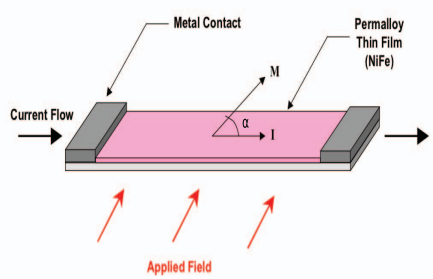

Figure 2: AMR Element with Applied Field H parallel to the surface of the permalloy. The direction of the current is perpendicular to the applied field. The magnetization vector makes an angle α with the current vector

aluminum stripes (barber poles), on top of the permalloy

strip at an angle of 45° to the strip axis. For sensors using barber poles arranged at an angle of $+45^\circ$ to the strip axis, the following expression for the sensor characteristic can be derived:

$$R = R_0 + \frac{\Delta R_0}{2} + \Delta R_0 \left(\frac{H}{H_0}\right)\sqrt{1 - \frac{H^2}{{H_0}^2}} \quad (11)$$

Likewise, for sensors using barber poles arranged at an angle of -45°, the equation derives to:

$$R = R_0 + \frac{\Delta R_0}{2} - \Delta R_0 \left(\frac{H}{H_0}\right)\sqrt{1 - \frac{H^2}{{H_0}^2}} \quad (12)$$

Equation of a balanced Wheatstone bridge is as follows.

$$\frac{R_4}{R_3} = \frac{R_2}{R_1} \quad (13)$$

If all four resistor values R_1, R_2, R_3 and R_4, the supply voltage V_s are known and the resistance of the galvanometer is high enough such that I_g is negligible, then the voltage across the bridge V_G can be found by working out the voltage from each potential divider and subtracting one from the other as shown in equation (14).

$$V_{BD} = V_G = \left(\frac{R_4}{R_3 + R_4} - \frac{R_2}{R_2 + R_1}\right) V_s \quad (14)$$

The resistances of a Wheatstone bridge are such that, resistances R_1 and R_4 increase, and resistances R_2 and R_3 decrease, due to the alignment of barber poles, when an external magnetic field is applied. The bridge is balanced by laser trimming. By comparing the mid-point voltages, absolute resistor tolerances are canceled and an extremely sensitive field detector can be made. Let α be the angle between the current flow and the resultant field for all the four resistances R_1, R_2, R_3 and R_4. Then,

$$R_1 = R_4 = R_0 + \frac{\Delta R_0}{2} + \Delta R_0 \left(\frac{H}{H_0}\right)\sqrt{1 - \frac{H^2}{{H_0}^2}} \quad (15)$$

$$R_2 = R_3 = R_0 + \frac{\Delta R_0}{2} - \Delta R_0 \left(\frac{H}{H_0}\right)\sqrt{1 - \frac{H^2}{{H_0}^2}} \quad (16)$$

Substituting R_1, R_2, R_3 and R_4 values from equation (15) and (16), and rearranging the terms we get,

$$V_{BD} = \left(\frac{\frac{\Delta R_0}{R_0}}{1 + \frac{\Delta R_0}{2R_0}}\right)\left(\frac{H}{H_0}\right)\left(\sqrt{1 - \frac{H^2}{{H_0}^2}}\right) V_s \quad (17)$$

In equation (17), since R_0 and ΔR_0 are material parameters. We define K as a material constant and is equal to:

$$K = \frac{\Delta R_0}{2R_0} \quad (18)$$

Substituting equations (9) and (18) in equation (17) and multiplying with the Op-Amp gain constant G we get,

$$V_{BD} = G\left(\frac{K}{1+K}\right)(\sin 2\alpha) V_s \quad (19)$$

REFERENCES

[1] J. Pucher, N. Korattyswaropam, N. Mittal, and N. Ittyerah, "Urban transport crisis in india," *Transport Policy*, vol. 12, no. 3, pp. 185 – 198, 2005.

[2] C. Cortes and V. Vapnik, "Support vector machines," *Machine Learning*, vol. 20, pp. 273–297, 1995.

[3] "Federal highway administration - vehicle types." US Department of Transportation. http://www.fhwa.dot.gov/policy/ohpi/vehclass.htm.

[4] Honeywell International Inc., 12001 Highway 55,Plymouth, MN 55441, *1, 2 and 3 Axis Magnetic Sensors HMC1051/HMC1052/HMC1053*. www.sparkfun.com/datasheets/IC/HMC105X.pdf.

[5] Hauser, Hans, Gnther Stangl, W. Fallmann, R. Chabicovskym, and K. Riedling. *Magnetoresistive Sensors*. Vol. 27. Retrieved September, 2002.

[6] EasySen, LLC., 401 North Coquillard Dr., South Bend, IN 46617, *SBT80, Multi-Modality Sensor Board for TelosB wireless motes*, Jan 2008. www.easysen.com/support/SBT80v2/DatasheetSBT80v2.pdf.

[7] A. S. Bhat, A. K. Deshpande, K. G. Deshpande, and K.V.S. Hari, "Vehicle detection and classification using magnetometer - data acquisition," tech. rep., 2011. http://eprints.iisc.ernet.in/43199/.

[8] S.-Y. Cheung and P. Varaiya, "Traffic surveillance by wireless sensor networks," research note, University of California, Berkeley, Jan 2007.

[9] Prateek G.V., Rajkumar V, Nijil K, and K.V.S. Hari, "Classification of Vehicles Using Magnetic Dipole Model" *in Proc. of IEEE TENCON*, nov 2012.

[10] MATLAB, *version 7.10.0 (R2010a)*. Natick, Massachusetts: The MathWorks Inc., 2010.